Asymmetric magnetic NOT gate and shift registers for high density data storage

Huang T. Zeng,[a] D. Read, L. O'Brien, J. Sampaio, E. R. Lewis, D. Petit, and R. P. Cowburn
Imperial College London, London SW7 2AZ, United Kingdom

(Received 17 May 2010; accepted 4 June 2010; published online 1 July 2010)

We have developed an asymmetric ferromagnetic NOT gate and shift register optimized on a square grid. This gives rise to a two-dimensional storage scheme built up by tessellating an elementary data unit, which is scalable down to very narrow wire widths. The areal footprint of each storage unit is $15F^2$, where F is the minimum feature size. We experimentally demonstrate NOT operations across a chain of three gates made from Permalloy with $F=60$ nm, and present a functional 15-gate, multichannel shift register with electrical injection, and optical readout. © *2010 American Institute of Physics*. [doi:10.1063/1.3457998]

There has been a great deal of interest in recent years focused on solid-state magnetic logic[1–6] and storage schemes.[7–9] Magnetic data storage promises a high density, nonvolatile memory unit that combines the performance of conventional random access memory with the low cost of magnetic disk drives. One such scheme involves linking a chain of logic elements (NOT gates) made from soft ferromagnetic nanowires to form a shift register.[10,11] The original design of these NOT gate shift registers was symmetrical about the input/output arms, enabling a bidirectional flow of data by choosing the sense of rotation of the external field[11] but the design had a large areal footprint in terms of F^2 (where F is the minimum feature size) making it unsuitable for high density data storage. We propose here an alternative gate geometry built up using a square mesh, where the width of each square (F) is also the nanowire width [see Fig. 1(a)]. This enables the creation of a storage scheme that is easily scalable to very narrow wire widths. An entire two-dimensional storage array can be built up by tessellating the element outlined in black in Fig. 1(a), which has an areal footprint of $15F^2$.

To gain an understanding of the switching processes for these gates, we have performed micromagnetic simulations using the OOMMF (Ref. 12) software on an $F=50$ nm gate with a thickness of 5 nm ($M_S=800\times10^3$ A/m, $A=13\times10^{-12}$ J/m, and (5,5,5) nm cell size). For the wire dimensions used here, transverse domain walls (TDWs) are the stable configuration.[13,14] TDWs have a distinct triangular shape, characterized by the DW charge [a measure of the divergence of magnetization, with head-to-head (HH) being positive and tail-to-tail (TT) being negative], and chirality (the sense of rotation of spins in the DW core).[15,16] Figure 1(b) shows the initial gate configuration with a HH-Down DW in the input arm (the core of the DW points downwards and the spins rotate clockwise (CW) across the wall, going left to right). Figure 1(c) shows a sequence of simulated configurations of the gate under a global, counter-clockwise (CCW) elliptical field (H) with x and y amplitudes of 70 and 300 Oe. The scaled field vector at each stage is indicated by the dark gray arrow in the background.

Since the magnetization in the core of the initial DW is parallel to the output arm, this DW sweeps past and annihilates at the stub, leaving behind a 90° DW at the intersection [c (i)]. This process can be understood in terms of DW interactions with T-structures.[17] The core magnetization of the residual 90° DW then undergoes CCW coherent rotation due to H, until it becomes parallel to the input arm and orthogonal to the output [(ii) to (iii)]. Further rotation beyond this point leads to a component of magnetization pointing in the opposite direction to the output effectively another 180° DW. This DW immediately depins from the intersection and exits the output arm [(iii) to (iv)], leaving the NOT gate magnetization fully reversed [panel (iv) is not an equilibrium configuration in the simulation but is included to illustrate the resultant configuration of the DW at the output]. Two things must be noted about the reversal process: First, the switching event is completed within half a field cycle of the global rotating field. Second, a HH DW with CW chirality at the input [Fig. 1(b)] has become a TT DW with CW chirality at the output (iv) a NOT gate operation reverses DW charge but preserves its chirality. We have also performed simulations (not shown here) for a HH-Up DW (CCW chirality) at the

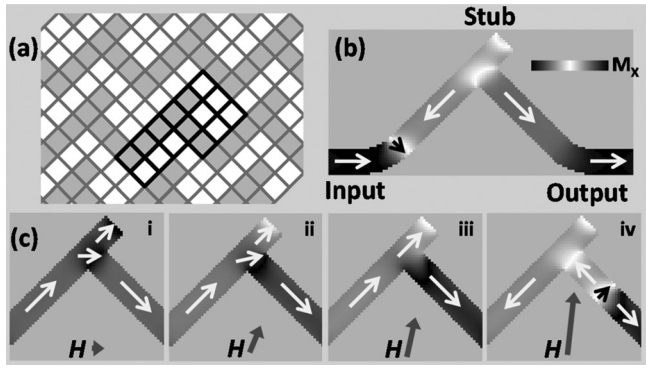

FIG. 1. (a) Schematic of the NOT gate design optimized on a square grid, with F=square width. The entire storage array can be constructed by tessellating the element highlighted in black (footprint=$15F^2$). (b) Micromagnetic simulation showing the initial gate configuration for $F=50$ nm. A HH-DW is present in the input arm with CW chirality. The system is driven by a globally rotating elliptical field. (c) Sequence of gate configurations illustrating the switching mechanism at different points in the field. The dark gray arrows in the background indicate the field vector.

[a]Electronic mail: huang.zeng@imperial.ac.uk.

input under identical field conditions, and again found the switching process preserves chirality and is complete within half a field cycle, despite the details of the micromagnetic mechanism being different. Due to the asymmetry in the gate design, data can only flow from left to right under a CCW field for a chain of gates, so data storage can only be achieved in first-in-first-out (FIFO) mode.

The inset in Fig. 3(a) shows a scanning electron microscope (SEM) image of an actual data storage array comprising of these NOT-gates, based on the template shown in Fig. 1(a). The devices presented here are fabricated via electron beam lithography on a Si substrate, followed by thermal evaporation of permalloy (Py) and a standard lift-off process. The resulting wires are 7 nm thick and 60 nm wide. A typical nanowire is characterized by two switching fields the nucleation field (H_N), which is the field needed to reverse the magnetization within a single domain wire; and the propagation field (H_P), which is the field required for a DW to move along the wire, overcoming intrinsic pinning due to wire roughness. For the wires presented here, $H_P=18\pm2$ Oe, $H_N=260\pm5$ Oe. With $F=60$ nm the areal footprint is 0.05 μm^2 per gate ($15F^2$), with further reductions possible at narrower wire widths using higher lithographic resolutions.

For the experiment, we first tested the operation of a single data line containing 3 gates. Data writing is performed by lithographing a 10 μm wide strip of Ti/Au (2 nm/160 nm) over the left end of the wire. The local Oersted field (H_{Local}) from a current pulse passing through the strip reverses the magnetization of the nanowire beneath it. Readout is achieved by placing the laser spot of a high sensitivity, spatially resolved magneto-optical Kerr effect (MOKE) magnetometer to the right of the shift register, and averaging the longitudinal Kerr signal over multiple field cycles. The two possible magnetization states of the nanowire are used to encode 0 (left) and 1 (right), which corresponds to low and high states in the MOKE output, respectively. During the write process, spikes in the MOKE output coincident with the current pulses are observed which are an experimental artifact and removed from the data. Additional variations in the MOKE signal due to Faraday rotation is also subtracted during postprocessing (see Ref. 11 for details).

Figure 2(a) shows data from the three-gate shift register in operation under a 12 Hz CCW drive field for a single write/read cycle. The clock frequency is limited due to the large impedance of the quadrupole electromagnet on the MOKE magnetometer. Given that the switching mechanism of the gate is a nucleation type process, occurring at high fields, it is feasible to envisage the gates switching within a very short timeframe (subnanosecond).[18] This means that drive frequencies of hundreds of megahertz are in principle possible, assuming the technical difficulties of producing such high frequencies drive fields can be overcome. A sequence of 180 mA current pulses (1 ms duration) is applied when $H_x=+(-)45$ Oe and $H_y=-(+)175$ Oe to create HH-Down (TT-Up) DWs. A simple three-bit sequence is written into the system over $3\times1/2$ field cycles, and read out over the following 3/2 cycles as the data is transmitted through the register. In the averaged MOKE signal (over 50 field cycles), this corresponds to no magnetic switching in the first 125 ms during the write interval, and transitions being recorded for 125 ms$<t<$250 ms during readout. The pulse

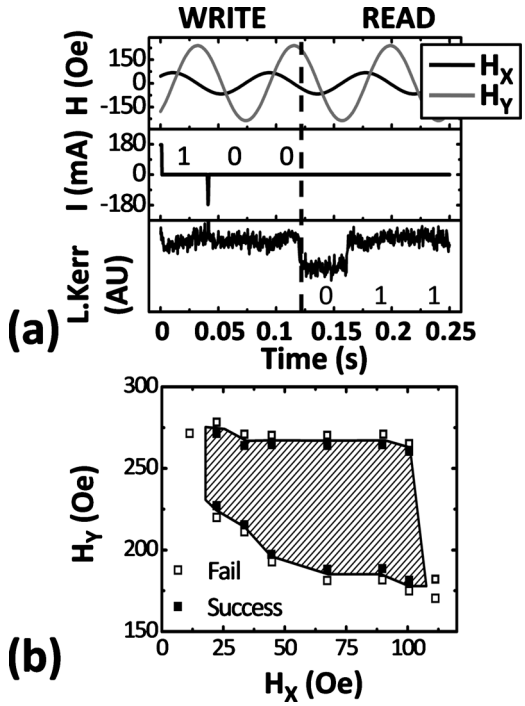

FIG. 2. (a) Experimental results showing three-gate data storage. Top panel: 12 Hz elliptical rotating field (H). Middle panel: pulse train used to inject DWs into the shift register, synchronized with H. Bottom panel: MOKE signal average over 50 field cycles measured after the gate. We observe no transitions during the write stage, and transitions after $t=125$ ms during readout. Data inversion occurs due to an odd number of gates. (b) Operating margin for the three-gate shift register.

sequence shown encodes 100, which becomes 011 upon readout. This reversal is a consequence of an odd number of inverting gates. Figure 2(b) shows the range of H_x, H_y in which the shift register operates. The absolute area of the operating margin is comparable to that for the first-generation gates which have been optimized for margin.[7]

The previous experiment involved passing data through a single channel but for a functional storage array, arbitrary data sequences must be passed through multiple channels without crosstalk[19,20] or desynchronization with the drive field. To demonstrate this we have lithographed three rows of five gates, spaced F apart, to create a 15-gate shift register. Arbitrary data sequences are injected simultaneously into each row using a multichannel waveform generator synchronized with H. Readout is performed by moving the MOKE spot between successive rows and averaging over 50 field cycles per row [see Fig. 3(a), with MOKE positions indicated by X]. An example of the multichannel gate operation is shown in Fig. 3(b). The data sequences 10 000, 10 100, and 00 100 are written into rows 1–3, respectively, over a duration of 5/2 field cycles, during which no transitions are observed in the MOKE signals across all data channels. In the subsequent 5/2 field cycles, readout occurs with 01 111, 01 011, and 11 011 being registered in rows 1 to 3 (inversion again due to odd number of gates). It will be noted that while the MOKE signal in rows 2 and 3 are exactly in phase, the transitions in row 1 are delayed by approximately 10 ms. This delay is a consequence of the readout geometry since the DWs in row 1 have to travel along a 30° upward diagonal to reach the MOKE spot, which requires the projection of H along 30° to exceed H_P. The results in Fig. 3 confirm that we can store arbitrary data sequences in multiple channels. No

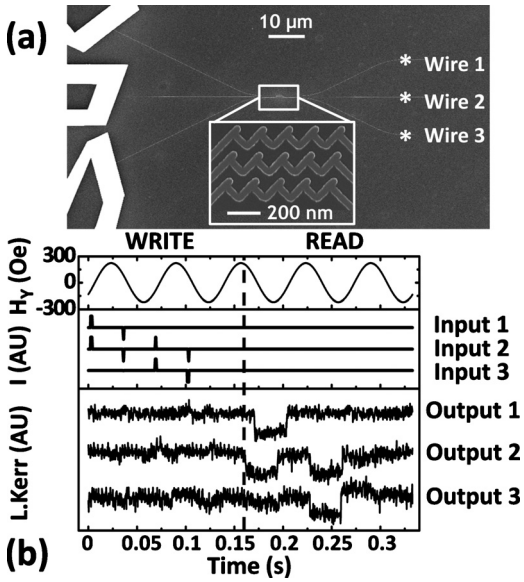

FIG. 3. (a) SEM image showing the setup for simultaneous injection of independent data sequences into three rows of five gates. Readout of each wire is obtained by moving the laser spot between the positions marked ∗. Inset: Image of the 15-gate data array, with $F=60$ nm. (b) Results showing write and read across all three data channels, with no crosstalk or dephasing observed. The delay in the MOKE transitions in wire 1 is a systematic effect due to the readout geometry.

appreciable cross-talk arising from magnetostatic coupling between DWs is observed, since the effect is weak compared to the drive-field of the gates. Additionally, reducing wire separation will not increase DW coupling as the wire widths are also scaled by the same amount, leading to a reduction in the DW magnetic charge that counteracts the effect of reduced separation.

To conclude, we have demonstrated the feasibility of shift registers based on asymmetric NOT gates optimized on a square mesh for data storage, with an areal footprint of $15F^2$. These gates are operated in FIFO mode, and are fully scalable down to very small wire widths. We studied the switching mechanisms across the gates using micromagnetic simulations, and found that DW chirality is preserved by the NOT operation. Multichannel data storage is demonstrated for gates with an areal footprint of $15F^2$ for $F=60$ nm using electrical input and optical readout, with negligible crosstalk observed.

[1]D. A. Allwood, G. Xiong, C. C. Faulkner, D. Atkinson, D. Petit, and R. P. Cowburn, Science **309**, 1688 (2005).
[2]R. P. Cowburn and M. E. Welland, Science **287**, 1466 (2000).
[3]A. Imre, G. Csaba, L. Ji, A. Orlov, G. H. Bernstein, and W. Porod, Science **311**, 205 (2006).
[4]J. Jaworowicz, N. Vernier, J. Ferre, A. Maziewski, D. Stanescu, D. Ravelosona, A. S. Jacqueline, C. Chappert, B. Rodmacq, and B. Dieny, Nanotechnology **20**, 215401 (2009).
[5]T. Hesjedal and T. Phung, Appl. Phys. Lett. **96**, 072501 (2010).
[6]M. H. Kryder and K. Chang Soo, IEEE Trans. Magn. **45**, 3406 (2009).
[7]D. A. Allwood, G. Xiong, M. D. Cooke, C. C. Faulkner, D. Atkinson, and R. P. Cowburn, J. Appl. Phys. **95**, 8264 (2004).
[8]M. T. Bryan, T. Schrefl, and D. A. Allwood, Appl. Phys. Lett. **91**, 142502 (2007).
[9]S. S. P. Parkin, M. Hayashi, and L. Thomas, Science **320**, 190 (2008).
[10]D. A. Allwood, G. Xiong, M. D. Cooke, C. C. Faulkner, D. Atkinson, N. Vernier, and R. P. Cowburn, Science **296**, 2003 (2002).
[11]L. O'Brien, D. E. Read, H. T. Zeng, E. R. Lewis, D. Petit, and R. P. Cowburn, Appl. Phys. Lett. **95**, 232502 (2009).
[12]The OOMMF code is available at http://math.nist.gov/oommf.
[13]Y. Nakatani, A. Thiaville, and J. Miltat, J. Magn. Magn. Mater. **290**, 750 (2005).
[14]R. D. McMichael and M. J. Donahue, IEEE Trans. Magn. **33**, 4167 (1997).
[15]O. Tchernyshyov and G. W. Chern, Phys. Rev. Lett. **95**, 197204 (2005).
[16]H. Youk, G. W. Chern, K. Merit, B. Oppenheimer, and O. Tchernyshyov, J. Appl. Phys. **99**, 08B101 (2006).
[17]D. Petit, A.-V. Jausovec, H. T. Zeng, E. Lewis, L. O'Brien, D. Read, and R. P. Cowburn, Phys. Rev. B **79**, 214405 (2009).
[18]J. Lu and X. R. Wang, J. Magn. Magn. Mater. **321**, 2916 (2009).
[19]M. Laufenberg, D. Bedau, H. Ehrke, M. Klaui, U. Rudiger, D. Backes, L. J. Heyderman, F. Nolting, C. A. F. Vaz, J. A. C. Bland, T. Kasama, R. E. Dunin-Borkowski, S. Cherifi, A. Locatelli, and S. Heun, Appl. Phys. Lett. **88**, 212510 (2006).
[20]L. O'Brien, D. Petit, H. T. Zeng, E. R. Lewis, J. Sampaio, A. V. Jausovec, D. E. Read, and R. P. Cowburn, Phys. Rev. Lett. **103**, 077206 (2009).